Bright Luminescent Silica Nanoparticles for Two-Photon Microscopy Imaging via Controlled Formation of 4,4′-Diethylaminostyryl-2,2′-bipyridine Zn(II) Surface Complexes

8 AUTHORS, INCLUDING:

Chantal Andraud
Claude Bernard University Lyon 1
223 PUBLICATIONS **3,054** CITATIONS

SEE PROFILE

Sophie Brasselet
Institut Fresnel
207 PUBLICATIONS **2,815** CITATIONS

SEE PROFILE

Christophe Copéret
ETH Zurich
284 PUBLICATIONS **6,958** CITATIONS

SEE PROFILE

Olivier Maury
Ecole normale supérieure de Lyon
169 PUBLICATIONS **3,448** CITATIONS

SEE PROFILE

Bright Luminescent Silica Nanoparticles for Two-Photon Microscopy Imaging via Controlled Formation of 4,4′-Diethylaminostyryl-2,2′-bipyridine Zn(II) Surface Complexes

Nuria Rendón,[†] Adrien Bourdolle,[†,‡] Patrice L. Baldeck,[§] Hubert Le Bozec,[||] Chantal Andraud,[‡] Sophie Brasselet,[*,⊥] Christophe Copéret,[*,†,#] and Olivier Maury[*,‡]

[†]Université de Lyon, C2P2, UMR 5265 (CNRS-CPE Lyon-Université Lyon 1), 43 Bd. Du 11 Novembre 1918, 69616 Villeurbanne Cedex, France

[‡]Université de Lyon, Laboratoire de Chimie, UMR 5182-CNRS-Ecole Normale Supérieure de Lyon-Universtité de Lyon 1, 46 allée d'Italie, 69007 Lyon, France

[§]Laboratoire de Spectrométrie Physique, Université Joseph Fourier, CNRS-UMR 5588, BP 87 F-38402 Saint Martin d'Hères, France

[||]UMR 6226 CNRS-Université de Rennes 1, Sciences Chimiques de Rennes, Campus de Beaulieu, 35042 Rennes Cedex, France

[⊥]Institut Fresnel, CNRS UMR 6133, Université Aix Marseille III, Ecole Centrale de Marseille, Domaine Universitaire St Jérôme, 13397 Marseille Cedex 20, France

[#]ETH Zürich, Department of Chemistry, Wolfgang-Pauli-Strasse 10, CH-8093 Zurich, Switzerland

Ⓢ Supporting Information

ABSTRACT: Silica nanoparticles with a surface functionalized by two-photon absorbing $(\equiv SiO)Zn(OSi(O^tBu)_3)$(**DEAS-bipy**) chromophores are prepared via surface chemistry controlled at the molecular level. This involves the grafting of $\{Zn[OSi(O^tBu)_3]_2\}_2$ on the surface silanols of a silica partially dehydroxylated at 700 °C followed by the coordination of **DEAS-bipy**. The spectroscopic and photophysical properties of the grafted species $(\equiv SiO)Zn(OSi(O^tBu)_3)$(**DEAS-bipy**)

compare well with that of the molecular model $\{$**DEAS-bipy**$Zn(OAc)_2\}$ with the advantage of allowing a high density of chromophores on a nanometric object (ca. 200 chromophores per silica particle of 12 nm). These particles are luminescent and exhibit a giant two-photon cross-section of about 90×10^3 GM; such two-photon brightness allows the imaging of a single nanoparticle using two-photon scanning microscopy.

KEYWORDS: luminescence, silica nanoparticles, Zn, bipyridine, imaging, two-photon scanning microscopy
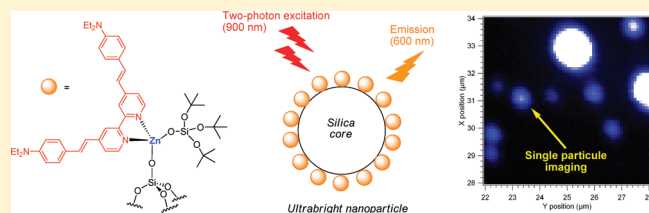
■ INTRODUCTION

Nowadays, two-photon absorption (TPA), a resonant third-order nonlinear process, has become an alternative excitation method enabling the promotion of chromophores to their excited state.[1] The TPA intrinsic advantages, i.e., long-wavelength and confocal absorption, combined with the larger accessibility of femto-second-tunable lasers, triggered the development of 3D resolved spectroscopy, microscopy, or photochemistry with a broad scope of applications[1,2] ranging from bioimaging, tracking, or sensing,[2a−d] photodynamic therapy,[2e−g] uncaging,[2h,i] optical limiting from the visible to the NIR,[2j−n] or microfabrication.[2o−q] All these advanced technological applications imposed their own molecular specifications, but all contributed to the design of chromophores featuring enhanced two-photon cross-section ($\sigma^{(2)}$ in Göppert-Mayer; 1 GM = 10^{-50} cm^4·s·photon^{-1}·molecule^{-1}). These engineering endeavors resulted in the preparation of optimized molecular dyes with σ^2 in the range of 1000 to several 10000 of GM.[3] To further improve the TPA efficiency, an

alternative strategy has consisted in taking advantage of local concentration effects by confining a large number of chromophores in nanoscale size objects, i.e., micellar nanoemulsion,[4] (hyperbranched or cyclic) oligomers,[5] dendrimers,[6] polymers,[7] and silica nanoparticles.[8] These latter particles have already been used as pH sensors;[8b] they can be multimodal, combining magnetic and TPEF properties,[8f] or can specifically target cancer cells, thanks to the additional coating of the silica particles' surface.[8h] All these particles were prepared using a rather similar method: the TPA dye was embedded into a silica matrix using Stöber or ORMOSIL emulsion sol−gel method and was consequently in interaction with this silica matrix. The above-mentioned nano-objects contain a large number of chromophores and consequently,

Chart 1. Schematic Representation of Luminescent Silica Nanoparticles Functionalized at the Surface with Two-Photon Excited Luminescent Zn(II) Complexes[a]

Model ligand and Zn(II) complex
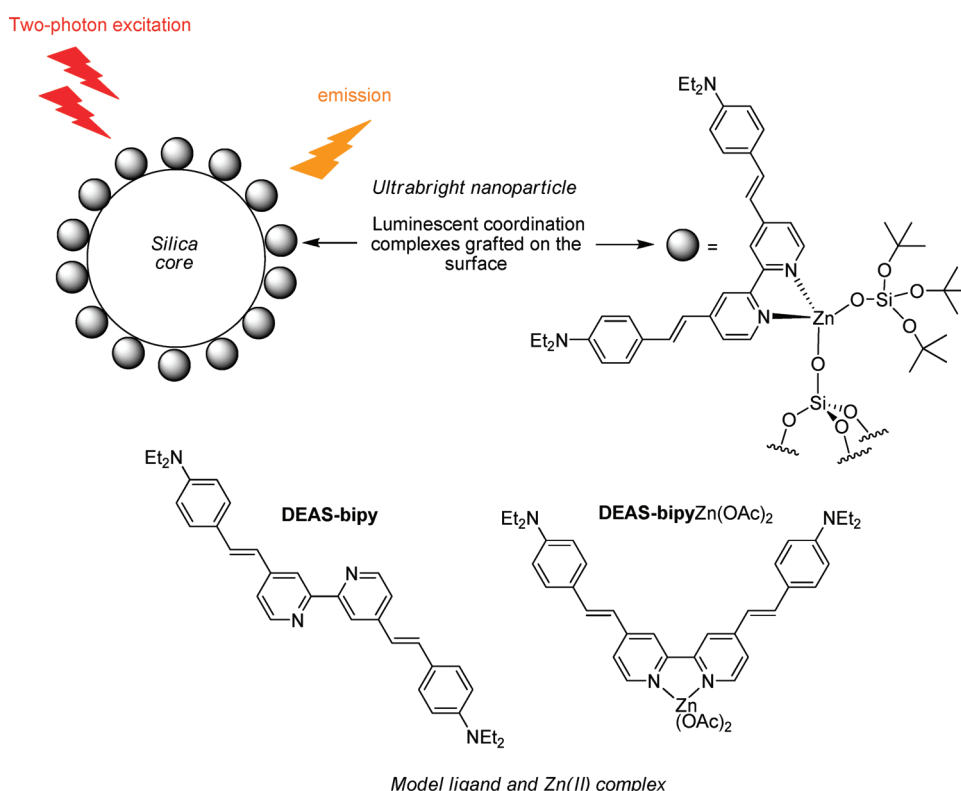
[a]Molecular formula of **DEAS-bipy** and **DEAS-bipy**Zn(OAc)$_2$.

using a simple additive model, exhibit giant two-photon cross-section up to 100000 GM.[4−8]

These nano-objects should therefore be extremely promising for two-photon microscopy bioimaging, which requires generally ultrahigh dilution where most often a single isolated nanoparticle is present in the focal volume of a microscope objective. Surprisingly, in spite of their giant cross-section, the observation of single nano-objects using a two-photon excitation is relatively scarce in the literature, and to the best of our knowledge, only four examples of the two-photon fluorescence correlation spectroscopy using nanodiamonds, polymer nanobeads, or quantum dots have already been reported.[7b,9]

Here, we describe a different approach, in which the chromophores are regularly dispersed at the surface of silica nanoparticles by means of surface reactions controlled at a molecular level, often termed Surface Organometallic Chemistry (SOMC).[10] This implies first a control of the OH density of oxide supports and then the selective grafting on these surface OH groups, which can be followed by a post-treatment or functionalization (reaction with ligands/molecules under thermal or photochemical conditions). Such an approach has been particularly successful to prepare the so-called single-site heterogeneous catalysts,[10,11] which usually display higher performances than both well-defined homogeneous catalysts and classical heterogeneous catalysts; this approach has also been used to control the dispersion of supported nanoparticles.[12]

Here, we apply this approach to obtain bright luminescent silica nanoparticles by controlling the density of Zn(II) centers

Scheme 1. Formation of $[(\equiv SiO)Zn(OSi(OtBu)_3)]$ by Grafting of $\{Zn[OSi(OtBu)_3]_2\}_2$ with the Isolated Silanols of $SiO_{2\text{-}(700)}$
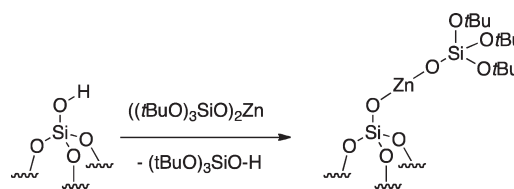
through grafting $\{Zn[OSi(OtBu)_3]_2\}_2$ on the surface silanols of 200 m$^2 \cdot$g^{-1} silica nanoparticles partially dehydroxylated at 700 °C (ca. 1 OH/nm^2 or 400 sites/nanoparticles) followed by a postfunctionalization via the coordination of 4,4′-(diethylaminostyryl)-2,2′-bipyridine (**DEAS-bipy**, Chart 1). At each step, the surface species were fully characterized by chemical analysis, FTIR, and CP-MAS NMR spectroscopy. The photophysical properties (absorption, emission, and two-photon absorption) of the nanoparticles are described and compared to that of the corresponding molecular ligand (**DEAS-bipy**) and complexes {**DEAS-bipy** Zn(OAc)$_2$},[13] whose second and third order NLO (nonlinear optical) properties have been widely studied.[14,15] This finally allowed the imaging of these nanoparticles using two-photon scanning microscopy, and their excellent brightness permitted one to reach single nanoparticle detection at low incident intensity.
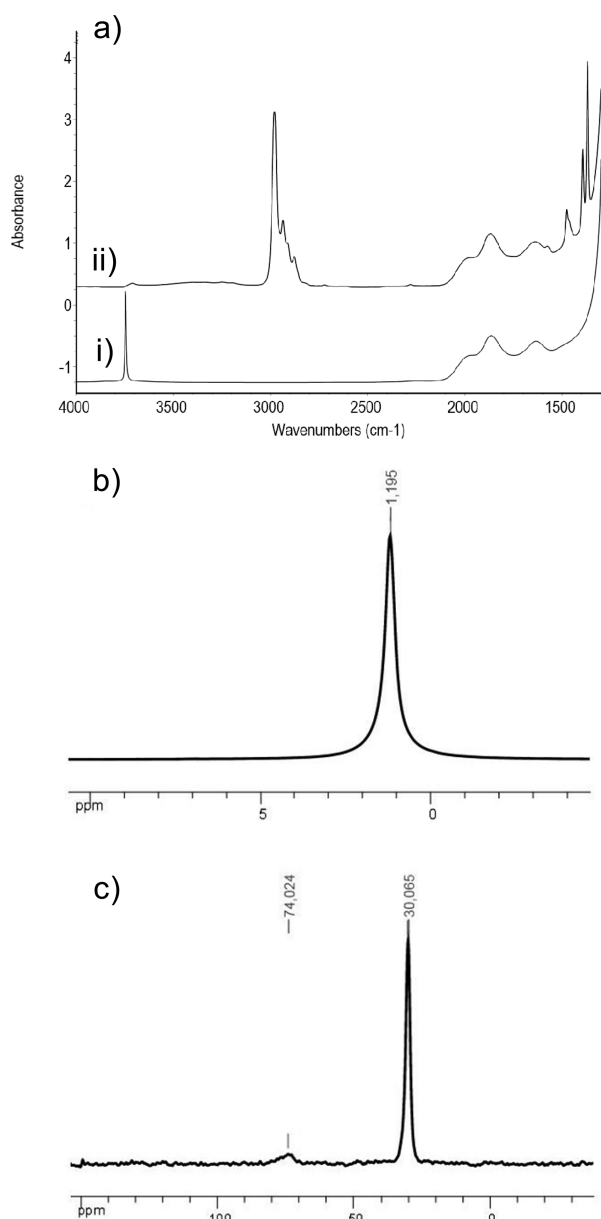
Figure 1. $[\mathbf{Zn(II)/SiO_2}]$ via grafting of $\{Zn[OSi(OtBu)_3]_2\}_2$ on $SiO_{2\text{-}(700)}$. (a) IR spectroscopy: (i) $SiO_{2\text{-}(700)}$ and (ii) after grafting of $\{Zn[OSi(OtBu)_3]_2\}_2$. (b) Proton magic angle spinning (MAS) solid-state NMR spectrum under a MAS frequency of 10 kHz; 8 scans were recorded at a recycle rate of 4 s. (c) CP-MAS carbon-13 solid-state NMR spectrum under a MAS frequency of 10 kHz; 32000 scans were recorded at a recycle rate of 2 s and a CP time of 2 ms.

Figure 2. $[\mathbf{DEAS\text{-}bipy/Zn(II)/SiO_2}]$ by reaction of $[\mathbf{Zn(II)/\ SiO_2}]$ with **DEAS-bipy**. (a) IR spectroscopy: DRIFT spectra before (i) and after (ii) the reaction. (b) Proton MAS solid-state NMR spectrum under a MAS frequency of 10 kHz; 8 scans were recorded at a recycle rate of 4 s. (c) CP-MAS carbon-13 solid-state NMR spectrum under a MAS frequency of 10 kHz; 26500 scans were recorded at a recycle rate of 2 s and a CP time of 2 ms.

■ RESULTS AND DISCUSSION

Synthesis of Luminescent Silica Nanoparticles. *Step 1: Controlled Doping of Silica with Zn(II) via Grafting of {Zn[OSi-(OtBu)_3]_2}_2 on SiO_{2-(700)} (Scheme 1)* . Reaction of $\{Zn[OSi(OtBu)_3]_2\}_2$,[16] on silica partially dehydroxylated at 700 °C, $SiO_{2\text{-}(700)}$, dispersed in pentane yielded a solid called $[\mathbf{Zn(II)/} \mathbf{SiO_2}]$ containing $1.81\%_{wt}$ of Zn, which corresponds to 0.27 mmol Zn/g of silica and thereby to the consumption of ca. 100% of the surface silanols (0.26 mmol OH/g for $SiO_{2\text{-}(700)}$).[17] This was confirmed by IR spectroscopy (Figure 1a) with the complete disappearance of the band at 3747 cm^{-1} associated with surface

silanol $\nu(SiO-H)$ bands: this reaction leads to the concomitant appearance of new IR bands in the 3000−2700 and 1500−1350 cm^{-1} regions, which were associated with the $\nu(C-H)$ and $\delta(C-H)$ of perhydrocarbyl ligands, respectively. Additional IR signals were also observed between 3000−3700 cm^{-1}, which were assigned to small amounts of residual OH groups interacting with perhydrocarbyl ligands (tBuO).[18] Moreover, 1.1 equiv. of $HOSi(OtBu)_3$ per grafted Zn was released during grafting according to quantitative NMR analysis of the supernatant, in agreement with the cleavage of one of the Zn−O bonds of $Zn[OSi(OtBu)_3]_2$ by surface silanols. Carbon elemental analysis on $[\mathbf{Zn(II)/SiO_2}]$ ($5.04\%_{wt}$) shows that the surface species contain an average of 15 ± 4 carbons per zinc, a value close to that expected for $[(\equiv SiO)Zn(OSi(OtBu)_3)]$, i.e., 12 C/Zn. The ^1H magic-angle spinning (MAS) solid-state NMR

Table 1. Photophysical Data in Solution and in the Solid State

| compounds	DEAS-bipy CH_2Cl_2	DEAS-bipyZnOAc$_2$ CH_2Cl_2	[DEAS-bipy/Zn(II)/ SiO$_2$] nanoparticle
λ_{max}/nm	397	432	460
ε/L·mol^{-1}·cm^{-1a}	40000	53000	
λ_{em}/nm	495	601	634
$\Phi_L{}^b$	0.11	0.36	
$\lambda^{(2)}{}_{max}$/nm ^{a,c}	770	890	
$\sigma^{(2)}$/GM ^{a,c}	225	435	87000^d

^{a} Determined in solution. ^{b} Coumarin-153 as standard (Φ = 0.45 in MeOH, λ_{ex} = 417 nm). ^{c} Coumarin-307 and fluorescein as reference. ^{d} Calculated value using an additive approximation with 200 active surface species.

spectrum displays a single resonance at 1.2 ppm associated with the methyl group of the tBuO ligand (Figure 1b) and the ^{13}C cross-polarization (CP) MAS solid-state NMR spectrum (Figure 1c) show two carbon signals at 74 and 30 ppm, which are assigned to the quaternary and the methyl carbons of the tBuO ligands. Overall, mass balance analysis, IR, and NMR spectroscopies are consistent with the formation of [($\equiv$SiO)Zn(OSi(OtBu)$_3$)], with a density of ca. 1 Zn(II)/nm^2 or ca. 400 Zn(II) centers per silica particles considering the mean size diameter of these silica nanoparticles, i.e., 12 nm.[19]

Step 2: Reaction of 4,4′-Diethylaminostyryl-2,2′-bipyridine with **[Zn(II)/SiO₂]**. Contacting a bright yellow-orange solution of **DEAS-bipy** (1 equiv) in dichloromethane with the white [**Zn(II)/SiO₂**] solid led to the rapid discoloration of the supernatant and to the red-orange coloration of the solid. After stirring the reaction mixture for 3 h at 25 °C, subsequent washing with CH$_2$Cl$_2$ and drying, a red-orange solid [**DEAS-BiPy/Zn(II)/ SiO₂**] was obtained, which contains 1.36%$_{wt}$ of Zn, 7.70%$_{wt}$ of C, and 0.75% of N. This elemental analysis corresponds to 31 ± 4 C/Zn and 2.6 ± 1 N/Zn and can be interpreted in terms of the formation of 55% of [($\equiv$SiO)Zn(OSi(OtBu)$_3$)(**DEAS-bipy**)] along with 45% of unreacted [($\equiv$SiO)Zn(OSi(OtBu)$_3$)]. Further increasing the reaction time did not change the outcome of this reaction. IR spectroscopy showed the incorporation of **DEAS-bipy** (Figure 2a). ^{1}H MAS NMR of [**DEAS-bipy/Zn(II)/SiO₂**] presents signals at 7.3 (CH$_{ar}$, CH=), 6.6 (CH$_{ar}$, CH=), 3.1 (CH$_2$), and 1.2 (CH$_3$), consistent with the presence of the **DEAS-bipy** and tBuO ligands (Figure 2b). Further characterization was performed by ^{13}C CP MAS spectroscopy (Figure 2c). The signals associated with **DEAS-bipy** and tBuO ligands are observed at the exception of the C$_2$ carbon expected at 156 ppm, which is replaced by a signal at 150.2 ppm, characteristic of the C$_2$ resonance of the 2,2′-bipyridyl ligand coordinated to Zn(II). In fact, a similar upfield shift is observed upon the coordination of **DEAS-bipy** to Zn(II).[13a] This was further corroborated using two zinc-free solids [**DEAS-bipy/SiO₂**] and [**DEAS-bipy/SiO₂-TMS**], prepared by adsorption of the **DEAS-bipy** ligand on either SiO$_{2-(700)}$ or a passivated silica covered with trimethylsilyl moieties in place of surface silanols,[20] respectively. In both cases, the corresponding solids have an orange-yellow color in marked contrast with [**DEAS-bipy/Zn(II)/SiO₂**] (orange-red), and they only display the typical C$_2$ resonance of free **DEAS-bipy** at 155.6 ppm (Figures S1−2, Supporting Information). This comparison

a)

b)
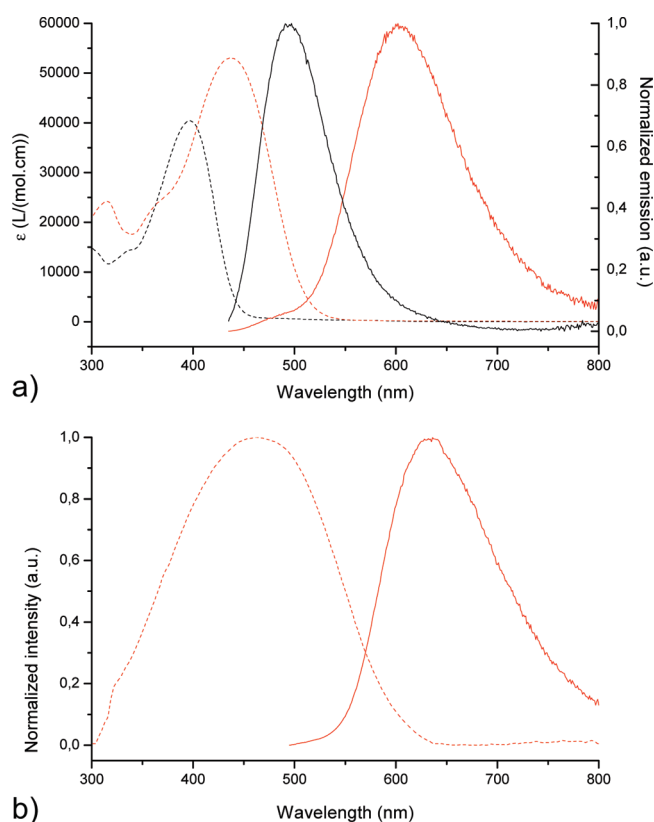
Figure 3. Absorption (dotted red lines) and emission (bold red line) of (a) **DEAS-bipy** (black line) and **DEAS-bipy**Zn(OAc)$_2$ (red) in CH$_2$Cl$_2$ solution and (b) [**DEAS-bipy/Zn(II)/SiO₂**] nanoparticles in the solid state.

unambiguously established the complete coordination of the **DEAS-bipy** ligand to Zn(II) centers in [**DEAS-bipy/Zn(II)/ SiO₂**]. Finally [**DEAS-bipy/Zn(II)/SiO₂**] was further characterized by absorption and emission spectroscopies, that are also in agreement with a complete Zn coordination of **DEAS-bipy** in the solid (vide infra). In contrast, **DEAS-bipy** coordinates only ca. 55% of Zn(II) surface sites (1.0 Zn/nm^2) because, when coordinated (adsorbed), the size of this ligand prevents access to some of the ligand-free Zn(II) sites. In fact, while it is not possible to precisely evaluate how this ligand lies on the surface of the silica nanoparticle, the projected surface area of coordinated **DEAS-bipy** is 1.7−2.3 nm^2 so that a silica nanoparticle of 12 nm diameter (450 nm^2 of external surface assuming a perfect sphere) should not be able to accommodate more than 190−270 ligands in agreement with experimental findings. Overall, each silica nanoparticle (ca. 12 nm) presents at the surface ca. 200 **DEAS-bipy**Zn(II) centers along with ca. the same amount of uncoordinated Zn(II) species.

Photophysical Properties in Solution. The photophysical properties of free **DEAS-bipy** and **DEAS-bipy**Zn(OAc)$_2$, used as a molecular model for [($\equiv$SiO)Zn(OSi(OtBu)$_3$)(**DEAS-bipy**)], were studied in dichloromethane solution, and the results are compiled in Table 1. Both compounds present broad intense and structureless absorption and emission in the visible (Figure 3, top)[13a,14c] assigned to intramolecular charge transfer (ICT) from the diethylamino donor group to the electron withdrawing bipyridine moieties.[14d] Since the coordination to Zn(II) reenforces the accepting character of the bipyridine ligand, both
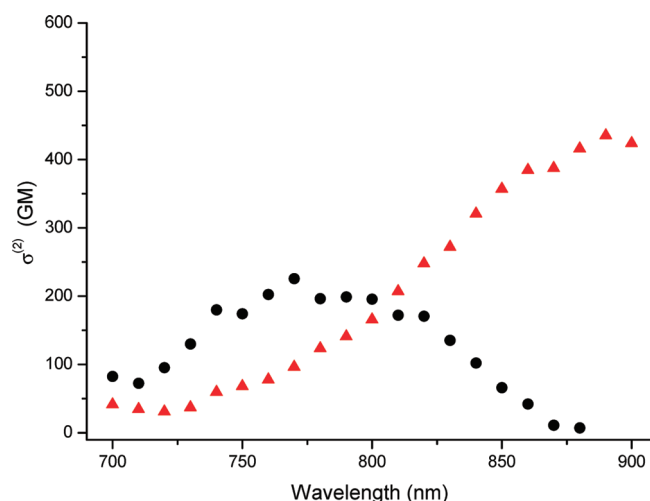
Figure 4. Two-photon cross-sections measured using the TPEF method in dichloromethane solution for **DEAS-bipy** (●) and **DEAS-bipy**-Zn(OAc)$_2$ (red triangle).

absorption and emission are red-shifted upon coordination ($\Delta\lambda^{abs}$-(CH$_2$Cl$_2$) = 35 nm, and $\Delta\lambda^{em}$(CH$_2$Cl$_2$) = 106 nm). In addition, a strong increase of the quantum yield efficiency from 0.11 to 0.36 is observed upon coordination due to the suppression of the free rotation around the intercycle bond reducing nonradiative de-excitation processes.[13a,14c] The two-photon cross-sections were determined by external calibration of the two-photon excitation fluorescence spectra (the TPEF method) with coumarin-153 as standard and are depicted in Figure 4. As expected, the two-photon excitation spectra match well the wavelength-doubled one photon absorption spectra indicating that the same excited state, here charge transfer excited states, are excited via one- or two-photon processes. The bathochromic shift induced by the coordination, initially observed in the absorption spectra, is also present in the two-photon excitation spectra with $\Delta\lambda^{(2)}$ = 120 nm. **DEAS-bipy** exhibits an important maximal two-photon cross-section ($\sigma^{(2)}$ = 225 GM at 770 nm) of the same order of magnitude as that of the related dibutylamino-functionnalized ligand ($\sigma^{(2)}$ = 278 GM at 780 nm) reported by Roberto and co-workers.[15c] In addition, Zn(II) coordination results in a 2-fold increase of the two-photon cross-section ($\sigma^{(2)}$ = 435 GM at 890 nm). Similar metal induced TPA exaltation has been already described,[15c,21] and the high NLO activity of **DEAS-bipy**Zn-(OAc)$_2$ makes such a family of complexes very attractive chromophores for the corresponding grafted entities.

Photophysical Properties in the Solid State. The photophysical properties of the nanoparticles were also investigated. Because of the loading of active species in the [**DEAS-bipy/Zn(II)/SiO$_2$**] solid (less than 10%$_{wt}$ of the solid), no dilution in neutral matrix is necessary. The spectrum is dominated by a broad absorption spectrum centered at 460 nm. Upon excitation between 400 and 550 nm, a single emission band centered at 634 nm is observed, similar to that of **DEAS-bipy**Zn(OAc)$_2$ (Figure 3, bottom). This confirms that every **DEAS-bipy** present at the surface of the nanoparticle is coordinated to a Zn(II) center. The two-photon cross-section of the nanoparticle cannot be experimentally determined using the TPEF method because it is not possible to disperse the nanoparticle in organic solvents. However, the cross-section of the [**DEAS-bipy/Zn(II)/SiO$_2$**] particle can be estimated using an additive model:[8e,f,h] the particle contains 200 NLO

active species [(≡SiO)Zn(OSi(OtBu)$_3$)(**DEAS-bipy**)] whose TPA cross-section can be estimated on the basis of the molecular model **DEAS-bipy**Zn(OAc)$_2$ to 435 GM. Consequently, the global grafted nanoparticle can be assumed to exhibit a giant TPA cross-section of ca. 90×10^3 GM, which falls in the same range as those reported for doped nano-objects[8] or quantum dots.[22]

Single Nanoparticle Imaging by Two-Photon Microscopy. The two-photon properties of isolated nanoparticles were studied in the solid state, simply by dispersing the powder on a microscope plate using a very low amount of material in order to favor single nanoparticle observation. Two-photon microscopy imaging was performed using a femto-second tunable Ti:sapphire laser (100 fs, 80 MHz) excitation source, in which the excitation wavelength was fixed at 900 nm at the maximum of the two-photon absorption spectrum (Figure 4). The excitation was focused by a high numerical aperture objective (NA 1.2, ×60), which was also used to collect the two-photon fluorescence signal from the nanoparticles. The emission, detected by avalanche photodiodes, was furthermore filtered spectrally in the visible region in order to avoid any scattering light from the incident laser. The scanning of the sample over a large area reveals bright luminescent spots, a signature of the presence of the [**DEAS-bipy/Zn(II)/SiO$_2$**] nanoparticles in regions of different sizes (Figure 5a). A close-up of this image (Figure 5b) shows that larger regions correspond to brighter aggregates (which are expected from the sample fabrication), while a large population is made of smaller spots corresponding to dispersed nanoparticles as shown in Figure 5c. The two-photon fluorescence signal from these isolated particles is stable in time over minutes in the intensity regime used for this measurement (60 μW averaged power at the focal spot of the microscope objective). Figure 5c shows that the image spot from a single nanoparticle exhibits a diameter of the order of the diffraction limit size of the objective (about 300 nm lateral, 600 nm axial), which is expected from an object of size lower than 100 nm typically. A spectral analysis of the luminescence of the smaller spots, measured from a spectrometer at the exit of the microscope, is depicted in Figure 5d and shows an emission band similar to that observed upon one-photon excitation (Figure 3b), which is also similar to that of the molecular complex **DEAS-bipy**Zn(OAc)$_2$ (Figure 3a), clearly establishing that the grafted chromophores are responsible for the nanoparticle NLO activity. Furthermore, the intensity of this single nanoparticle emission exhibits a quadratic dependence with the incident laser power. These results unambiguously establish that the measured signals originate from the two-photon excited emission of [**DEAS-bipy/Zn(II)/SiO$_2$**] nanoparticles.

Since a large population of spots in the recorded images exhibits a diffraction-limited size, we studied the level of signal from this population considering that they may represent isolated nanoparticles (considering their size, the presence of a few-particle aggregates, not detectable in the diffraction limit size, would lead to an overestimation of the efficiency by a factor of 2 to 8). The level of signal emitted from these diffraction-limited spots is reproducible over a large population of nano-objects, as shown by the histogram of maximum intensities measured on 47 particles (Figure 5e). Since the two-photon fluorescence signal is proportional to the volume of the particle (and therefore its diameter to the power 3), a deviation of a factor of 2 in the signal leads to a deviation of less than a factor of 1.3 for the particle size, which shows the homogeneity of the detected population. The average
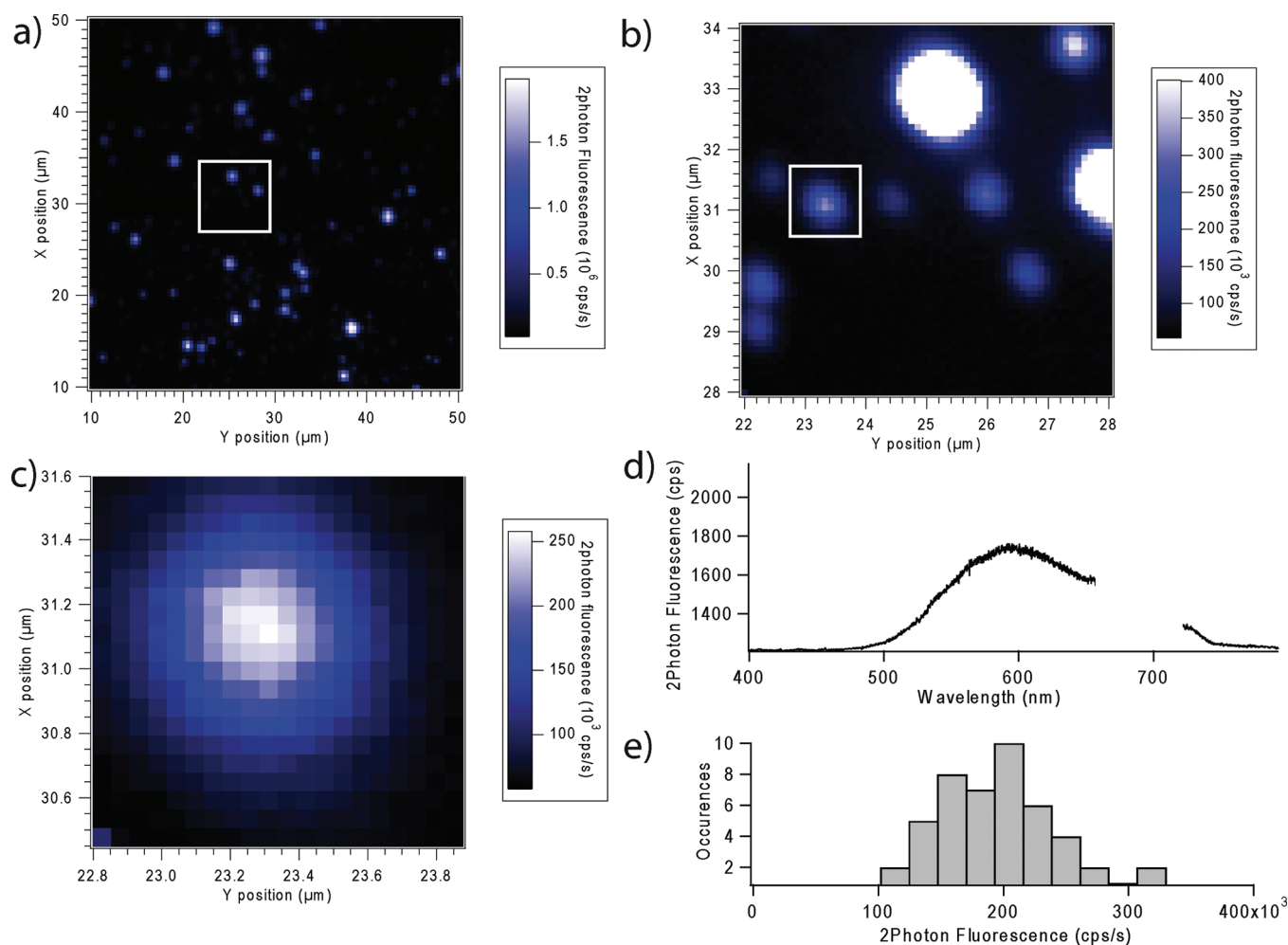
Figure 5. (a) Two-photon fluorescence scanning image of a collection of nanoparticles dispersed on a microscope plate in a 40 μm range ($\lambda^{(2)}_{ex}$ = 900 nm). (b) Close-up at a 6 μm range showing the presence of aggregates and of isolated nanoparticles. (c) Close-up of a single nanoparticle (exhibiting a diffraction-limited spot). The square a and b represent the zoomed-in region. (d) Emission spectrum of a single nanoparticle (the removed part of the curve corresponds to a spectral region where scattering by the incident laser remained unfiltered in the spectral detection path). (e) Histogram of the intensity maxima measured over 47 identified single nanoparticles imaged in the same incident intensity conditions. Incident averaged power at the entrance of the objective: 60 μW.

two-photon fluorescence intensity signal over this population is typically 2×10^5 photons/s when illuminated by a 60 μW averaged power at the focal spot of the microscope objective (which corresponds to a 70 kW·cm^{-2} intensity). This signal is about 3 to 4 orders of magnitudes higher than the emission previously measured from single molecules of rhodamine derivatives in the same instrumental conditions (for which $\sigma^{(2)}$ is about 150 GM) at a similar excitation intensity (see Experimental Section for the calculation details).[23,24] It also surpasses by 2 to 3 orders of magnitude the signal previously obtained in single nanoparticles of similar sizes, made from the conjugated polymer PFPV for which $\sigma^{(2)}$ was estimated to about 10^4 GM (see Experimental Section).[7b] The observed efficiency is also consistent with the number of active molecules per nanoparticles, on the basis of a pure additive model and supposing that the observed diffraction limit spot is made of isolated single nanoparticles. The final single particle signal makes these nanoparticles, some of the brightest ones already described in the literature.

■ CONCLUSIONS

Overall, here was presented a novel design, the synthesis and the complete characterization of silica nanoparticles functionalized by two-photon absorbing ($\equiv$SiO)Zn(OSi(OtBu)$_3$)(**DEAS-bipy**) surface chromophores, which are bright and luminescent nano-objects of ca. 10 nm. This was possible via a controlled grafting of a Zn(II) molecular complex directly at the surface of silica nanoparticles dehydroxylated at 700 °C by a selective reaction with the surface silanols, whose density is fixed to ca. 1 OH per nm^2, followed by coordination of **DEAS-Bipy** on these isolated Zn(II) centers. This approach, usually called surface organometallic chemistry and reserved for the preparation of supported single-site catalysts,[10] allows the formation of silica nanoparticles having ca. 200 Zn(II) centers coordinated to **DEAS-Bipy**, which thus display giant two-photon cross-sections (about 90×10^3 GM) and which can thereby be successfully imaged using two-photon scanning microscopy. The very high two-photon brightness of these particles unambiguously validate the new site isolation surface grafting synthetic approach and make these nano-objects

Table 2. Comparison of Two-Photon Fluorescence Efficiencies of Single Nanoparticles[a]

	I (W/cm^2)	measured TPEF signal (ph/s)	fluorescence signal ratio relative to [**DEAS-bipy** /Zn(II)/SiO$_2$] particles
[**DEAS-bipy** /Zn(II)/SiO$_2$] particles[b]	70×10^3	2×10^5	1
tetramethylrhodamine single molecules[c]	1000×10^3	7×10^3	~1/6500
Rh6G single molecules[d]	3×10^6	1×10^4	~1/50000
PFPV 10 nm nanoparticles[e]	300×10^3	3×10^3	~1/375−1/1120

[a] In these works similar excitation source are used: incident wavelength 800 nm, 100 fs, 80 MHz repetition rate. [b] In our experiment, the excitation area is of diameter 300 nm, with an averaged incident power of 60 μW. [c] $\sigma^{(2)}$ = 150 GM at 800 nm for anologous Rhodamine B. The fluorescence signal from a single isolated tetramethylrhodamine molecule is estimated to be about 7 photons/ms for an illumination intensity of 1000 kW/cm^2.[23] [d] The fluorescence signal from a single isolated Rhodamine 6G molecule is estimated to be about 200 photons/20 ms for an illumination power of 3 mW using a similar focusing objective as in our experiment (therefore, a diameter of 300 nm is used in the calculation of the incident intensity).[24] [e] 10 nm size PFPV nanoparticles ($\sigma^{(2)}$ = 10^4 GM at 800 nm)[7b] are said to emit about 10^6 photons before photobleaching, with a decay time estimated to be about 100−300 s. The two relative fluorescence signals are given for these two decay times. The incident power is 260 μW with similar focusing conditions as in our work.

very promising for bioimaging applications. To that long-term end, high brightness is necessary but not sufficient, and many other requirements such as stability, solubility, targeting, etc. will have to be taken into account and are actually in progress in our groups.

■ EXPERIMENTAL SECTION

General Procedure. All organometallic syntheses were carried out under dry and oxygen free Ar using either standard Schlenk or glovebox techniques. For the syntheses and the treatments of the surface complexes, all reactions were carried out using high vacuum lines (1.34 Pa) and glovebox techniques. 4,4′-(Diethylaminostyryl)-2,2′-bipyiridine (**DEAS-bipy**),[13a] Zn(OAc)$_2$(**DEAS-bipy**),[13a] and Zn[OSi(OtBu)$_3$]$_2$[16] were synthesized according to the literature procedure. Silica (Aerosil Degussa, 200 m^{2}g^{-1}) was compacted with distilled water, calcined at 500 °C under air for 2 h, and treated under vacuum (1.34 Pa) at 500 °C for 12 h and then at 700 °C for 4 h (support referred to as SiO$_{2-(700)}$ and containing 0.26 mmol OH/g as measured by titration with MeMgCl[25]). Pentane was distilled from NaK[25] under N$_2$. C$_6$D$_6$ (SDS) and benzene were distilled from sodium benzophenone ketyl under N$_2$. Elemental analyses were performed at the University of Bourgogne, Dijon (C and N), and at the Mikroanalythisches Labor Pascher.

Infrared Spectroscopy. Infrared spectra were recorded on a Nicolet 550-FT by using an infrared cell equipped with CaF$_2$ windows, allowing *in situ* studies. Typically, 16 scans were accumulated for each spectrum (resolution, 2 cm^{-1}).

Nuclear Magnetic Resonance Spectroscopy. *Solution Nuclear Magnetic Resonance Spectroscopy.* Liquid state NMR spectra were recorded in C$_6$D$_6$ using a Bruker AC 300 and DRX 500 spectrometer and referenced to the residual protonated solvent peak (^{1}H δ_H = 7.15 ppm).

Solid State Nuclear Magnetic Resonance Spectroscopy. All solid state NMR spectra were recorded under MAS on a Bruker Avance 500 spectrometer with a conventional double resonance 4 mm CP-MAS probe. The MAS frequency was set to 10 or 12.5 kHz for the experiments reported here. The samples were introduced in a 4 mm zirconia rotor in the glovebox and tightly closed. Proton and carbon chemical shifts are reported in ppm downfield from liquid SiMe$_4$ (0 ppm).

Reaction of [Zn(OSi(OtBu)$_3$)$_2$] with SiO$_{2-(700)}$. Preparation of **[Zn(II)/SiO$_2$]**. A mixture of {Zn[OSi(OtBu)$_3$]$_2$}$_2$ (154 mg, 0.13 mmol) and SiO$_{2-(700)}$ (500 mg, 0.13 mmol SiOH) dispersed in pentane (20 mL) was stirred at 25 °C for 3 h. The resulting white solid was washed three times with pentane (around 10 mL), and the resulting white powder [**Zn(II)/SiO$_2$**] was dried under vacuum (1.34 Pa) at 25 °C for 2 h. All the filtrate solutions were collected and analyzed by quantitative ^{1}H NMR spectroscopy (in C$_6$D$_6$) using Cp$_2$Fe (49 mg, 152 μmol, 10 H) as

internal standard: 164 μmol of HOSi(OtBu)$_3$ (1.1 H for the HOSi-(OtBu)$_3$) was formed during grafting (1.1 equiv of HOSi(OtBu)$_3$/Zn$_{surf}$). ^{1}H MAS NMR: 1.2. ^{13}C CP MAS NMR: 74 and 30 ppm. Elemental analysis: 1.81 ± 0.05%$_{wt}$ Zn, 5.04 ± 0.10%$_{wt}$ C, 15 ± 4 C/Zn (12 expected).

Reaction of [Zn(II)/SiO$_2$] with DEAS-bipy. Preparation of **[DEAS-BiBy/Zn(II)/ SiO$_2$]**. A mixture of [**Zn(II)/SiO$_2$**] (500 mg, 0.14 mmol Zn) and **DEAS-BiPy** (70 mg, 0.14 mmol) in CH$_2$Cl$_2$ (20 mL) was stirred at 25 °C for 3 h. The resulting orange solid was washed three times with CH$_2$Cl$_2$, filtered, and dried under high vacuum (1.34 Pa) at 25 °C for 1 h, thus yielding [**DEAS-bipy/Zn(II)/ SiO$_2$**]. ^{1}H MAS NMR: 7.3 (CHar, CH=), 6.6 (CHar, CH=), 3.1 (CH$_2$), 1.2 (CH$_3$). ^{13}C CP MAS NMR: 150.2 (C2), 149.4 (C4, C6, C12), 138.2 (C8), 128.5 (C10), 122.6 (C3, C5, C7, C9), 111.1 (C11), 43.5 (C13), 30.4 (OtBu), 10.2 (C14) ppm. Elemental analysis: 1.36 ± 0.05%$_{wt}$ Zn, 7.70 ± 0.10%$_{wt}$ C, 31 ± 4 C/Zn (12 expected), 0.75 ± 0.4%$_{wt}$ N, 2.57 N/Zn.

Preparation of [DEAS-bipy/SiO$_2$]. A solution of **DEAS-bipy** (30 mg, 0.06 mmol) in CH$_2$Cl$_2$ (8 mL) was added to SiO$_{2-700}$ (300 mg, 0.078 mmol OH), which immediately turned orange. The solvent was removed under reduced pressure giving an orange solid. Extensive washing with CH$_2$Cl$_2$ does not alter the orange color. ^{1}H MAS NMR: 6.8 (CHar, CH=), 3.1 (CH$_2$), 0.9 (CH$_3$). ^{13}C CP NMR: 155.6 (C2), 148.0 (C4, C6, C12), 132.8 (C8), 128.3 (C10), 120.9 (C3, C5, C7, C9), 111.1 (C11), 43.4 (C13), 10.3 (C14). Elemental analysis: C: 6.38%; H: 0.64%; N: 0.82%.

Preparation of [DEAS-bipy/Passivated_SiO$_2$]. To a slurry of SiO$_{2-700}$ (400 mg) in pentane (6 mL), hexamethyldisilazane (0.25 mL) was added. After stirring the resulting suspension at room temperature for 4 h, the solvent was removed under reduced pressure, and the solid (passivated silica)[19] was dried under high vacuum (1.34 Pa) at 150 °C for 8 h. ^{1}H MAS NMR: −0.3 (SiMe$_3$). Then, a solution of **DEAS-bipy** (20 mg, 0.04 mmol) in CH$_2$Cl$_2$ (6 mL) was added to the passivated silica (200 mg), which immediately turned orange. The solvent was removed under reduced pressure and dried under high vacuum for 2 h. ^{1}H MAS NMR: 6.4 (CHar, CH=), 3.1 (CH$_2$), 1.5 (CH$_3$), −0.2 (SiMe$_3$). ^{13}C CP NMR: 155.3 (C2), 149.3 (C12), 147.5 (C4), 145.5 (C6), 132.6 (C8), 125.7 (C10), 123.6 (C9), 121.3 (C7), 119.6 (C5), 112.0 (C3), 110.9 (C11), 43.0 (C13), 11.6 (C14), −2.6 (SiMe$_3$). Elemental analysis: C: 4.77%; H: 0.59%; N: 0.49%.

Luminescence. The luminescence spectra were measured using a Horiba-Jobin Yvon Fluorolog-3 spectrofluorimeter, equipped with a three slit double grating excitation and emission monochromator with dispersions of 2.1 nm/mm (1200 grooves/mm). The steady-state luminescence was excited by unpolarized light from a 450 W xenon CW lamp and detected by a red-sensitive Hamamatsu R928 photomultiplier tube. Spectra were reference corrected for both the excitation source light intensity variation (lamp and grating) and the emission spectral response (detector and grating). Measurements were performed at an

3234

dx.doi.org/10.1021/cm2010852 |*Chem. Mater.* 2011, 23, 3228–3236

angle of 90° for the diluted solution in a 10 mm quartz cuvette and at an angle of 22° (front face detection) in a solid-state microholder for solids. In the case of the [**DEAS-bipy/Zn(II)/SiO₂**] solid, measurements were also carried out under inert atmosphere in airtight cells at an angle of 45°.

Two-Photon Excited Luminescence Measurements. The TPA cross-section spectra were obtained by up-conversion fluorescence using a Ti: sapphire femtosecond laser in the range 700−900 nm. The excitation beam (5 mm diameter) is focalized with a lens (focal length 10 cm) at the middle of the fluorescence cell (10 mm). The fluorescence, collected at 90° to the excitation beam, was focused into an optical fiber (diameter 600 μm) connected to an Ocean Optics S2000 spectrometer. The incident beam intensity was adjusted to 50 mW in order to ensure an intensity-squared dependence of the fluorescence over the whole spectral range. The detector integration time was fixed to 1s. Calibration of the spectra was performed by comparison with the published 700−900 nm Coumarin-307 two photon absorption spectrum[60] (Coumarin-307 quantum yield 0.56 in ethanol). The measurements were carried out at room temperature in CH_2Cl_2 at a concentration of 10^{-4} M.

Two-Photon Microscopy Imaging. The two-photon microscope imaging uses an excitation source from a Ti:Sa laser (pulse width, 100 fs; repetition rate, 80 MHz) set at a wavelength of 900 nm. The light is focused on the sample using a water immersion high numerical aperture objective (NA 1.2, ×60), after reflection on a two-photon dichroic mirror. The fluorescence emission, collected by the same objective, is filtered spectrally using a large visible band-pass filter (350−600 nm) and focused on an avalanche photodiode working in the photon counting mode with a dark rate of 200 counts per second. The sample is mounted on a piezo-electric scanner which can scan up to 200 × 200 μm areas, with a step of down to 1 nm. The imaging setup leads to a lateral resolution of about 300 nm and to an axial resolution of about 600 nm. Therefore, a lateral scan step of 100 nm is chosen on the piezo-electric scanner.

Comparison of TPA Efficiency of Single Nanoparticles with Existing Systems. The comparison of two-photon fluorescence efficiencies of single nanoparticles with existing systems is obtained considering the quadratic dependence of this effect relative to the incident intensity. The comparison is given in Table 2. In order to calculate the normalized fluorescence signal used for comparison with [**DEAS-bipy** /Zn(II)/ SiO₂] particles (last column), all measured two-photon fluorescence signals are divided by the squared intensity I^2.

■ ASSOCIATED CONTENT

ⓢ **Supporting Information.** CP-MAS ¹H and ¹³C NMR spectra of [**DEAS-bipy/SiO₂**] and [**DEAS-bipy/Passivated_SiO₂**] (PDF). This material is available free of charge via the Internet at http://pubs.acs.org.

■ AUTHOR INFORMATION

Corresponding Author
*E-mail: Sophie.brasselet@Fresnel.fr (S.B.); ccoperet@inorg.chem.ethz.ch (C.C.);olivier.maury@ens-lyon.fr (O.M.).

■ REFERENCES

(1) For reviews, see(a) Sumalekshmy, S.; Fahrni, C. J. *Chem. Mater.* **2011**, *23*, 483–500. (b) Kim, H. M.; Cho, B. R. *Chem. Asian J.* **2011**, *6*, 58–69. (c) Ogilby, P. R. *Chem. Soc. Rev.* **2010**, *39*, 3181–3209. (d) Kim, H. M.; Cho, B. R. *Chem. Commun.* **2009**, 153–164. (e) Pawlicki, M.; Collins, H. A.; Denning, R. G.; Anderson, H. L. *Angew. Chem., Int. Ed.* **2009**, *48*, 3244–3266. (f) Andraud, C.; Maury, O. *Eur. J. Inorg. Chem.* **2009**, 4357–4371. (g) Kim, H. M.; Cho, B. R. *Acc. Chem. Res.* **2009**, *42*, 863–872. (h) He, G. S.; Tan, L.-S.; Zheng, Q.; Prasad, P. N. *Chem.*

Rev. **2008**, *108*, 1245–1330.(i) Andraud, C.; Fortrie, R.; Barsu, C.; Stéphan, O.; Chermette, H.; Baldeck P. L. In *Photoresponsive Polymers II Book Series: Advances in Polymer Sciences*; Marder, S., Lee, K.-S., Eds.; Springer: New York, 2008; Vol. 214, pp 149−203; (j) Nyman, E. S.; Hynninen, P. H. *J. Photochem. Photobiol. B* **2004**, *73*, 1–28. (k) Detty, M. R.; Gibson, S. L.; Wagner, S. J. *J. Med. Chem.* **2004**, *47*, 3897–3915.

(2) For recent examples, see(a) Wang, X.; Nguyen, D. M.; Yanez, C. O.; Rodriguez, L.; Ahn, H.-Y.; Bondar, M. V.; Belfield, K. D. *J. Am. Chem. Soc.* **2010**, *132*, 12237–12239. (b) Picot, A.; D'Aléo, A.; Baldeck, P. L.; Grichine, A.; Duperray, A.; Andraud, C.; Maury, O. *J. Am. Chem. Soc.* **2008**, *130*, 1532–1533. (c) Barsu, C.; Cheaib, R.; Chambert, S.; Queneau, Y.; Maury, O.; Cottet, D.; Wege, H.; Vial, J.-C.; Douady, J.; Bretonnière, Y.; Andraud, C. *Org. Biomol. Chem.* **2010**, *8*, 142–150. (d) Kim, M. K.; Lim, C. S.; Hong, J. T.; Han, J. H.; Jang, H.-Y.; Kim, H. M.; Cho, B. R. *Angew. Chem., Int. Ed.* **2010**, *49*, 364–367. (e) Ke, H.; Wang, H.; Wong, W.-K.; Mak, N.-K.; Kwong, D. W. J.; Wong, K.-L.; Tam, H.-L. *Chem. Commun.* **2010**, *46*, 6678–6680. (f) Nielsen, C. B.; Arnbjerg, J.; Johnsen, M.; Jorgensen, M.; Ogilby, P. R. *J. Org. Chem.* **2009**, *74*, 9094–9104. (g) Andrasik, S. J.; Belfield, K. D.; Bondar, M. V.; Hernandez, F. E.; Morales, A. R.; Przhonska, O. V.; Yao, S. *ChemPhysChem* **2007**, *8*, 399–404. (h) Pirrung, M. C.; Dore, T. M.; Zhu, Y.; Rana, V. S. *Chem. Commun.* **2010**, *46*, 5313–5315. (i) Warther, D.; Bolze, F.; Léonard, J.; Gug, S.; Specht, A.; Puliti, D.; Sun, X.-H.; Kessler, P.; Lutz, Y.; Vonesch, J.-L.; Winsor, B.; Nicoud, J.-F.; Goeldner, M. *J. Am. Chem. Soc.* **2010**, *132*, 2585–2590. (j) Bouit, P.-A.; Kamada, K.; Feneyrou, P.; Berginc, G.; Toupet, L.; Maury, O.; Andraud, C. *Adv. Mater.* **2009**, *21*, 1151–1154. (k) Hales, J. M.; Cozzuol, M.; Screen, T. E. O.; Anderson, H. L.; Perry, J. W. *Opt. Express* **2009**, *17*, 18478–18488. (l) Zhou, G.; Wong, W.-Y.; Poon, S.-Y.; Ye, C.; Lin, Z. *Adv. Funct. Mater.* **2009**, *19*, 531–544. (m) Westlund, R.; Glimsdal, E.; Lindgren, M.; Vestberg, R.; Hawker, C.; Lopes, C.; Malmström, E. *J. Mater. Chem.* **2008**, *18*, 166–175. (n) Girardot, C.; Cao, B.; Mulatier, J.-C.; Baldeck, P. L.; Chauvin, J.; Riehl, D.; Delaire, J. A.; Andraud, C.; Lemercier, G. *ChemPhysChem* **2008**, *9*, 1531–1535. (o) Pham, T. A.; Kim, D.-P.; Lim, T.-W.; Park, S.-H.; Yang, D.-Y.; Lee, K.-S. *Adv. Funct. Mater.* **2006**, *16*, 1235–1241. (p) Xing, J.-F.; Chen, W.-Q.; Gu, J.; Dong, X.-Z.; Takeyasu, N.; Tanaka, T.; Duan, X.-M.; Kawata, S. *J. Mater. Chem.* **2007**, *17*, 1433–1438. (q) Wang, I.; Bouriau, M.; Baldeck, P. L.; Martineau, C.; Andraud, C. *Opt. Lett.* **2002**, *27*, 1348–1350.

(3) For selected examples, see(a) Albota, M.; Bejonne, D.; Brédas, J.-L.; Ehrlich, J. E.; Heikal, A. A.; Hess, S. E.; Kogej, T.; Levin, M. D.; Marder, S. R.; McCord-Maighon, D.; Perry, J. W.; Röckel, H.; Rumi, M.; Subramaniam, G.; Webb, W. W.; Wu, X.-L.; Xu, C. *Science* **1998**, *281*, 1653–1656. (b) Yang, W. J.; Kim, D. Y.; Jeong, M.-Y.; Kim, H. M.; Jeon, S.-J.; Cho, B. R. *Chem Commun* **2003**, 2618–2619. (c) Bartholomew, G. P.; Rumi, M.; Pond, S. J. K.; Perry, J. W.; Tretiack, S.; Bazan, G. C. *J. Am. Chem. Soc.* **2004**, *126*, 11529–11542. (d) Oliviera, S. L.; Corrêa, D. S.; Misoguti, L.; Constantino, C. J. L.; Aroca, R. F.; Zilio, S. C.; Mendonça, C. R. *Adv. Mater.* **2005**, *17*, 1890–1893. (e) Yang, W.J.; Kim, D. Y.; Jeong, M.-Y.; Kim, H. M.; Lee, Y. K.; Fang, X.; Jeon, S.-J.; Cho, B. R. *Chem.—Eur. J.* **2005**, *11*, 4191–4198. (f) Chung, S. J.; Zheng, S.; Odani, T.; Beverina, L.; Fu, J.; Padilha, L. A.; Biesso, A.; Hales., J. M.; Zhan, X.; Schmidt, K.; Ye, A.; Zojer, E.; Barlow, S.; Hagan, D. J.; VanStryland, E. W.; Yi., Y.; Shuai, Z.; Pagani, G. A.; Bredas, J.-L.; Perry, J. W.; Marder, S. R. *J. Am. Chem. Soc.* **2006**, *128*, 14444–14445. (g) Mongin, O.; Porres, L.; Charlot, M.; Katan, C.; Blanchard-Desce, M. *Chem.—Eur. J.* **2007**, *13*, 1481–1498. (h) Zheng, S.; Leclercq, A.; Fu, J.; Beverina, L.; Padilha, L. A.; Zojer, E.; Schmidt, K.; Barlow, S.; Luo, J.; Jiang, S.-H.; Jen, A. K. Y.; Yi, Y.; Shuai, Z.; Van Stryland, E. W.; Hagan, D. J.; Bredas, J.-L.; Marder, S. R. *Chem. Mater.* **2007**, *19*, 432–442. (i) Easwaramoorthi, S.; Shin, J. Y.; Cho, S.; Kim, P.; Inokuma, Y.; Tsurumaki, E.; Osuka, A.; Kim, D. *Chem.—Eur. J.* **2009**, *15*, 12005–12017.

(4) Maurin, M.; Vurth, L.; Vial, J.-C.; Baldeck, P. L.; Marder, S. R.; Van der Sanden, B.; Stephan, O. *Nanotechnology* **2009**, *20*, 235102.

(5) (a) Screen, T. E. O.; Thorne, J. R. G.; Denning, R. G.; Bucknall, D. G.; Anderson, H. L. *J. Am. Chem. Soc.* **2002**, *124*, 9712–9713. (b) Rath, H.; Sankar, J.; Prabhu,-Raja, V.; Chandrashekar, T. K.; Nag, A.;

Goswami, D. *J. Am. Chem. Soc.* **2005**, *127*, 11608–11609. (c) Kim, K. S.; Lim, J. M.; Osuka, A.; Kim, D. *J. Photochem. Photobiol., C* **2008**, *9*, 13–28.

(6) (a) Mongin, O.; Krishna, T. R.; Werts, M. H. V.; Caminade, A.-M.; Majoral, J.-P.; Blanchard-Desce, M. *Chem. Commun.* **2006**, 915–917. (b) Mongin, O.; Pla-Quitana, A.; Terenziani, F; Drouin, D.; Le Droumaguet, C.; Caminade, A.-M.; Majoral, J.-P.; Blanchard-Desce, M. *New J. Chem.* **2007**, *31*, 1354–1367. (c) Terenziani, F.; Parthasarathy, V.; Pla-Quitana, A.; Maishal, T.; Caminade, A.-M.; Majoral, J.-P.; Blanchard-Desce, M. *Angew. Chem., Int. Ed.* **2009**, 8691–8694.

(7) (a) Drobizhev, M.; Stepanenko, Y.; Rebane, A.; Wilson, C. J.; Screen, T. E. O.; Anderson, H. L. *J. Am. Chem. Soc.* **2006**, *128*, 12432–12433. (b) Wu, C.; Szymanski, C.; Cain, Z.; Mc Neil, J. *J. Am. Chem. Soc.* **2007**, *129*, 12904–12905.

(8) (a) Bertazza, L.; Celotti, L.; Fabbrini, G.; Loi, M. A.; Maggini, M.; Mancin, F.; Marcuz, S.; Menna, E.; Muccini, M.; Tonellato, U. *Tetrahedron* **2006**, *62*, 10434–10440. (b) Kim, S.; Pudavar, A.; Prasad, P. N. *Chem. Commun.* **2006**, 2071–2073. (c) Kim, S.; Pudavar, H. E.; Bonoiu, A.; Prasad, P. N. *Adv. Mater.* **2007**, *19*, 3791–3795. (d) Kim, S.; Ohulchanskyy, T. Y.; Pudavar, H. E.; Pandey, R. K.; Prasad, P. N. *J. Am. Chem. Soc.* **2007**, *129*, 2669–2675. (e) Wen, X.; Li, M.; Wang, Y.; Zhang, J.; Fu, L.; Hao, R.; Ma, Y.; Ai, X. *Langmuir* **2008**, *24*, 6932–6936. (f) Chelebaeva, E.; Raehm, L.; Durand, J.-O.; Guari, Y.; Larionova, J.; Guérin, C.; Trifonov, A.; Willinger, M.; Thangavel, K.; Lascialfari, A.; Mongin, O.; Mir, Y.; Blanchard-Desce, M. *J. Mater. Chem.* **2010**, *20*, 1877–1884. (g) Li, L.; Tian, Y.; Yang, J.; Sun, P.; Kong, L.; Wu, J.; Zhou, H.; Zhang, S.; Jin, B.; Tao, X.; Jiang, M. *Chem. Commun.* **2010**, *46*, 1673–1675. (h) Shao, G.; Han, R.; Ma, Y.; Tang, M.; Xue, F.; Sha, Y.; Wang, Y. *Chem.—Eur. J.* **2010**, *16*, 8647–8651.

(9) Berland, K. M.; So, P. T. C.; Gratton, E. *Biophys. J.* **1995**, *68*, 694–701. Levi, V.; Ruan, Q. Q.; Gratton, E. *Biophys. J.* **2005**, *88*, 2919–2928. Hui, Y. Y.; Zhang, B.; Chang, Y.-C.; Chang, C.-C.; Chang, H.-C.; Hsu, J.-H.; Chang, K.; Chang, F.-H. *Opt. Express* **2010**, *18*, 5896–5905.

(10) (a) Copéret, C.; Chabanas, M.; Petroff Saint-Arroman, R.; Basset, J.-M. *Angew. Chem., Int. Ed.* **2003**, *42*, 156–181. (b) Guzman, J.; Gates, B. C. *Dalton Trans.* **2003**, 3303–3318. (c) Fujdala, K. L.; Brutchey, R. L.; Tilley, T. D. *Top. Organomet. Chem.* **2005**, *16*, 69–115. (d) Thomas, J. M.; Raja, R.; Lewis, D. W. *Angew. Chem., Int. Ed.* **2005**, *44*, 6456–6482. (e) Tada, M.; Iwasawa, Y. *Coord. Chem. Rev.* **2007**, *251*, 2702–2716.

(11) (a) Ballard, D. H. R. *Adv. Catal.* **1975**, *23*, 263–325. (b) Marks, T. *Acc. Chem. Res.* **1992**, *25*, 57–65. (c) Copéret, C. *Dalton Trans.* **2007**, 5498–5504.

(12) Gajan, D.; Guillois, K.; Delichère, P.; Basset, J.-M.; Candy, J.-P.; Caps, V.; Copéret, C.; Lesage, A.; Emsley, L. *J. Am. Chem. Soc.* **2009**, *131*, 14667–14669.

(13) (a) Maury, O.; Guégan, J.-P.; Renouard, T.; Hilton, A.; Dupau, P.; Sandon, N.; Toupet, L.; Le Bozec, H. *New J. Chem.* **2001**, *25*, 1553–1566. (b) Viau, L.; Maury, O.; Le Bozec, H. *Tetrahedron Lett.* **2004**, *45*, 125–128.

(14) For second order NLO, see(a) Hilton, A.; Renouard, T.; Maury, O.; Le Bozec, H.; Ledoux, I.; Zyss, J. *Chem. Commun.* **1999**, 2521–2522. (b) Sénéchal, K.; Maury, O.; Le Bozec, H.; Ledoux, I.; Zyss, J. *J. Am. Chem. Soc.* **2002**, *124*, 4561–4562. (c) Maury, O.; Viau, L.; Sénéchal, K.; Corre, B.; Guégan, J.-P.; Renouard, T.; Ledoux, I.; Zyss, J.; Le Bozec, H. *Chem.—Eur. J.* **2004**, *10*, 4454–4466. (d) Baccouche, A.; Peigne, B.; Ibersiene, F.; Hammoutene, D.; Boutarfaïa, A.; Boucekkine, A.; Feuvrie, C.; Maury, O.; Ledoux, I.; Le Bozec, H. *J. Phys. Chem. A* **2010**, *114*, 5429–5438.

(15) For third order NLO, see(a) Feuvrie, C.; Maury, O.; Le Bozec, H.; Ledoux, I.; Morrall, J. P.; Dalton, G. T.; Samoc, M.; Humphrey, M. G. *J. Phys. Chem. A* **2007**, *111*, 8980–8985. (b) Mazzucato, S.; Fortunati, I.; Scolaro, S.; Zerbetto, M.; Ferrante, C.; Signorini, R.; Pedron, D.; Bozio, R.; Locatelli, D.; Righetto, S.; Roberto, D.; Ugo, R.; Abbotto, A.; Archetti, G.; Beverina, L.; Ghezzi, S. *Phys. Chem. Chem. Phys.* **2007**, *9*, 2999–3005. (c) Dragonetti, C.; Balordi, M.; Colombo, A.; Roberto, D.; Ugo, R.; Fortunati, I.; Garbin, E.; Ferrante, C.; Bozio, R.; Abbotto, A.; Le Bozec, H. *Chem. Phys. Lett.* **2009**, *475*, 245–249.

(16) Su, K.; Tilley, T. D.; Sailor, M. J. *J. Am. Chem. Soc.* **1996**, *118*, 3459–3468.

(17) For other examples of grafting of metal siloxide precursors on silica, see(a) Brutchey, R. L.; Mork, B. V.; Sirbuly, D. J.; Yang, P.; Tilley, T. D. *J. Mol. Catal. A: Chem.* **2005**, *238*, 1. (b) Holland, A. W.; Li, G. T.; Shahin, A. M.; Long, G. J.; Bell, A. T.; Tilley, T. D. *J. Catal.* **2005**, *235*, 150–163. (c) Ruddy, D. A.; Tilley, T. D. *Chem. Commun.* **2007**, 3350–3352.

(18) Rhers, B.; Salameh, A.; Baudouin, A.; Quadrelli, E. A.; Taoufik, M.; Copéret, C.; Lefebvre, F.; Basset, J.-M.; Solans-Monfort, X.; Eisenstein, O.; Lukens, W. W.; Lopez, L. P. H.; Sinha, A.; Schrock, R. R. *Organometallics* **2006**, *25*, 3554–3557.

(19) http://www.aerosil.com/lpa-productfinder/page/productsbytext/faces/productde.

(20) Anwander, R.; Nagl, I.; Widenmeyer, M.; Engelhardt, G.; Groeger, O.; Palm, C.; Roeser, T. *J. Phys. Chem. B* **2000**, *104*, 3532.

(21) (a) Righetto, S.; Rondena, S.; Locatelli, D.; Roberto, D.; Tessore, F.; Ugo, R.; Quici, S.; Roma, S.; Korystov, D.; Srdanov *J. Mater. Chem.* **2006**, *16*, 1439–1444. (b) Grisanti, L.; Sissa, C.; Terenziani, F.; Painelli, A.; Roberto, D.; Tessore, F.; Ugo, R.; Quici, S.; Fortunati, I.; Garbin, E.; Ferrante, C.; Bozio, R. *Phys. Chem. Chem. Phys.* **2009**, *11*, 9450–9457.

(22) (a) Larson, D. R.; Zipfel, W. R.; Williams, R. M.; Wise, F. W.; Clark, S. W.; Bruchez, M. P.; Webb, W. W. *Science* **2003**, *300*, 1434–1436. (b) Pu, S.-C.; Yang, M.-J.; Hsu, C.-C.; Lai, C.-W.; Hsieh, C.-C.; Lin, S. H.; Cheng, Y.-M.; Chou, P.-T. *Small* **2006**, *2*, 1308–1313. (c) Clapp, A. R.; Pons, T.; Medintz, I. L.; Delehanty, J. B.; Melinger, J. S.; Tiefenbrunn, T.; Dawson, P. E.; Fisher, B. R.; O'Rourke, B.; Mattoussi, H. *Adv. Mater.* **2007**, *19*, 1921–1926.

(23) Sonnleitner, M.; Schütz, G. J.; Schmidt, T. *Chem. Phys. Lett.* **1999**, *300*, 221–226.

(24) Farrer, R. A.; Previte, M. J. R; Olson, C. E.; Peyser, L. A.; Fourkas, J. T.; So, P. T. C. *Opt. Lett.* **1999**, *24*, 1832–1834.

(25) Note that these compounds react violently with water and should be handled under inert atmosphere (absence of air and water).